中國機械工程學刊第四十二卷第一期第 43~50 頁(民國一百一十年)
Journal of the Chinese Society of Mechanical Engineers, Vol.42, No.1, pp 43~50 (2021)

Research on Flow Field Characteristics of an Artificial Seawater Spray Chamber

Liang-Cai Li*, Yue Yin*, Bo Wan* and Yi-Gang Luan **

Keywords：nozzle experiment, spray chamber, numerical simulation

ABSTRACT

Air-intake filters can filter out salt aerosols in the ocean atmosphere, which plays a key role in improving quality of air intake for marine gas turbine. To carry out precise experiment study on air-intake filters for gas turbine and its improved design, ocean atmosphere simulating in laboratory conditions is needed. Thus, an artificial seawater spray chamber with spraying nozzles is designed to produce aerosols, which is similar to salt aerosols in real ocean atmosphere. Droplet concentration uniformity is an important indicator to measure performance of artificial seawater spray chamber. In this article, experimental method and CFD technology were both used to explore impact of nozzle performance and arrangement on droplet concentration uniformity in the spray field. To obtain more accurate numerical simulation data, an experiment was carried out before simulation to measure atomizer angle and particle size distribution of the spray, which will be used in real artificial seawater spray chamber. Experiment data was taken into CFD software, set as the initial boundary conditions. In the numerical simulation, changing number and arrangement of nozzles, gas-particle two-phase flow field in different schemes have been calculated. Those data can be used as references in designing real artificial seawater spray chamber.

INTRODUCTION

Ocean atmosphere contains salt which exist in form of aerosol, intake air of ocean vessels usually has to be desalinated. Many large ships are equipped with gas turbine power equipment. For its great amount of intake air, gas turbine engine has strict requirement in desalination (Gan, 2006). It means designers have to simulate the ocean atmosphere under laboratory conditions, which will be helpful for further study in marine gas-water separators in numerical simulations and experiment study. It can also provide reliable data for designers in designing high-performance marine gas-water separator. However, how to simulate ocean atmosphere better is always a research focus and spraying is an effective way. There are many factors that can affect the concentration uniformity of spray field, including structure of the spray chamber, performance of the nozzles, number and arrangement of the nozzles (Li, 2006). At present, researches on the atomizing nozzle are mainly carried out by ways of combining theoretical analysis and experimental methods. In theoretical analysis, unstable wave theory has been used to explain the atomization mechanism and process. Nozzle is an important part of combustion chamber, its operating characteristics affect the performance of combustion chamber directly. Many scholars have done some in-depth experiment studies on fuel nozzle. Bulzan et al. (1996) carried out some experiments on mist combustion flow field in the single-stage axial cyclone quartz glass cylinder chamber. Oil droplets velocity distribution and airflow, along with the oil bead size distribution, have been tested using LDA and PDPA. Soltani et al. (2005) conducted some experimental studies on particles and gas velocity distribution in a single-stage cyclone combustor in both cold and combustion conditions, in which particle SMD, particle size and flux distribution have been measured. Cai et al. (2005) did some further researches about impact of oil mist swirling mist distribution and characteristics by measuring mist chamber combustion flow field in a single-stage axial cyclone model. It shows that the mist velocity distribution influence greatly on swirl flow field. Fu and Mongia et al. (2005) measured the two-phase combustion flow field in a square combustion chamber, obtained three-dimensional velocity and turbulence intensity distribution of vapor and liquid phases, oil bead size and flux distribution. Jeng et al. (2004) measured the SMD and droplet size distribution in different axial positions of the CFM56 swirl cup from GE Company, using two-dimensional PDPA.

Paper Received December, 2018. Revised February, 2020, Accepted July, 2020, Author for Correspondence: Yi-Gang Luan.

* *College of Power and Energy Engineering, Harbin Engineering University, Harbin, Heilongjiang 150001 China;*

** *College of Power and Energy Engineering, Harbin Engineering University, Harbin 150001, China. Corresponding author, Shandong-313@163.com.*

Flow field in spray chamber is a typical two-phase flow field. Turbulence models used in the gas-liquid two-phase calculations include Dispersed Phase Model, Hybrid Model, Euler Model, VOF model and Level Set model (Sun, 2006). Discrete Phase Model is mainly used for droplet flow and bubble flow calculation. It assumes that volume of the droplet or bubble will not become too large and it will distribute evenly in the continuous phase. That means the local particle volume concentration ratio is less than 10% (Zhang, 2009). Discrete Phase Model belongs to Euler-Lagrange type model. In calculating the droplet, the gas is continuous phase and the droplet is dispersed phase. By calculating the continuous phase, velocity, turbulent kinetic energy and other information of the flow field can be obtained. In the Lagrangian coordinates, trajectory of single droplet is integrated (Tambe et al., 2005). Trajectory of single droplet will be obtained after the force in continuous phase field and other physical quantity have been calculated. Turbulence calculations are carried out under the concept of statistical average. Turbulent flow field obtained in the calculation is also the flow field in sense of the average. Therefore, it's unable to reproduce the turbulent flow field accurately in the calculation (Ma et al., 2001). It means the calculation of single droplet trajectory has no practical significance. It is nonsense only if the statistical laws of droplet motion are obtained after a large number of droplet trajectories are calculated (Zhang et al. 2006). Discrete Phase Model is the model which can simulate the movement of a large number of droplets by calculation.

EXPERIMENTAL RESEARCH

Atomizer angle measurement

In artificial seawater spray chamber, spray angle of the nozzle affects distribution of droplet directly in atomization chamber. Therefore, measurements of the atomization nozzle cone angle and characteristics study under different working conditions are significant (Zhang, 2006). Nozzle used in the test is shown in Figure 1. The conical nozzle is adjustable pressure type. Operating pressure range is from 10Kpa to 50Kpa.

Fig. 1. The test nozzle

Atomizing angle is one of the design parameters, which usually will not change too much with pneumatic varying, hydraulic or other conditions. Size of the atomizing angle will affect working conditions of the equipment. Therefore, type of nozzle should be chosen carefully according to the practical working requirements. In this article, considering need for designing the spray chamber, atomizing angle of a selected nozzle has been tested under different working conditions. During the test, atomizing angles are measured by taking photos while the nozzle is working under stable condition (Rao et al., 1976).

In this study, the atomizing angle has been measured under seven different pressure conditions: 15KPa、20KPa、25KPa、30KPa、35KPa、40KPa、45KPa.The angle data is shown in Table 1.

Table 1. Nozzle spray angle data

	1	2	3	4	5	6	7
Pressure (KPa)	15	20	25	30	35	40	45
Angle (°)	27.3	27.8	28.2	27.6	28.7	28.3	29.4

PDA Experiment

In order to measure performance of the nozzle, a variety of quantitative indicators have been proposed, such as average diameter, characteristics diameter. In field of spray science, Mugele and Evans proposed a concept called droplet average diameter. The average diameters used most commonly are length mean diameter, surface area mean diameter, volume mean diameter and Sauter average diameter (Liao et al., 2007).

When studying the spraying, Sauter average diameter is the first choice in preliminary analysis. Two kinds of mean diameter are adopted here. The first one is Length Average Diameter, its expression is:

$$D_{10} = \int_{D_{Min}}^{D_{Max}} DdN \Big/ \int_{D_{Min}}^{D_{Max}} dN \tag{1}$$

The second one is Sauter Mean Diameter, customarily indicated by symbol SMD or D_{32}

$$D_{32} = \frac{\sum n_i d_i^3}{\sum n_i d_i^2} \tag{2}$$

The PDA system used in this test is shown below, in Figure 2 and 3.

Fig. 2. Laser generator part of the PDA system

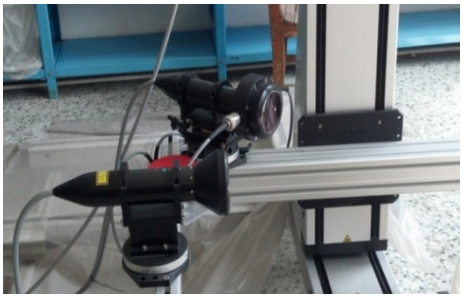

Fig. 3. Laser probe of the PDA system

In this test, several different working conditions with different pressures or liquid flow rate are chosen. D_10, D_32 and the maximum particle size measured in tests. Data are obtained in the section of 355mm away from the nozzle exit (Zheng et al., 2010).

1. Tests under constant flow rate conditions:

In the constant flow conditions, 7 groups of tests, numbered 1-7, have been carried out. Results are shown below, in Figure 4.

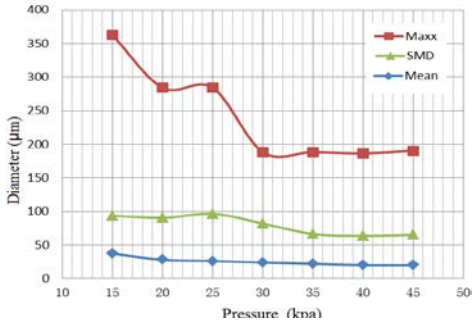

Fig. 4. The variation of the average diameter along with the pressure

In the Fig 4, Mean、Maxx、SMD represents length average diameter, maximum diameter of the droplet group and Sauter Mean Diameter respectively.

As shown, the maximum particle size changes most obviously. When the pressure is 15KPa, the maximum particle size is 362.5 microns; when it increases to 30KPa, the maximum size reduced to 188.2 microns. When it increases continuously, the maximum particle size has no significant changes with pressure variation. It means the increasing of pressure can improve atomization within a certain range. When the pressure increases from 15KPa to 25KPa, the SMD is almost unchanged. When it increases from 25KPa to 40KPa, the SMD decreased obviously. After 40KPa, it remains stable. The length average has similar variations. Data obtained from the experiment shows that pressure is one of the main factors that can impact atomization effect. In low-pressure conditions, the atomized particle size decreases significantly with pressure increase. However, when it increases to a certain value, particle size changes slightly before it remains stable.

2. Tests under constant pressure conditions:

In the constant pressure conditions, 9 tests numbered 8-16 were carried out. In the experiment, the average diameter is measured under different conditions with the increasing flow rate of water. Results are shown below in Figure 5.

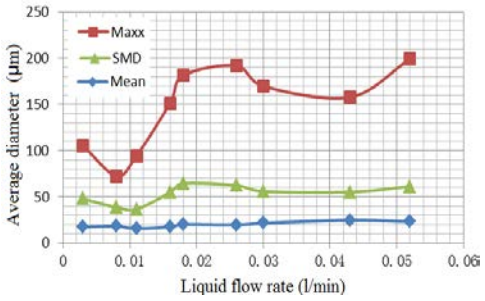

Fig. 5. The variation of the average diameter along with the liquid flow rate

It's obvious that with water flow rate increase, the maximum size shows an overall upward trend. When the flow rate is 0.008L/Min, the maximum particle size is 72.4 microns. And increasingly it reached 192.3 microns at 0.026 L/Min. After slightly decrease, when 0.052L / Min, the maximum particle size is uptrend again. It means the liquid flow rate has an influence nozzle atomization effect. For larger the flow rate, the atomization effect becomes worse.

Although length average diameter and Sauter average diameter increase with the increasing of flow rate, they still have some distinctions (Fuster et al., 2009). In given flow rate range, minimum value of the length average diameter is 15.5 microns, the corresponding flow rate is 0.011L/Min. The maximum value is 24.7 microns, and corresponding flow rate is 0.043L/Min. Changes of the length average diameter is not obvious with the variation of flow rate. However, SMD variation is little different. When liquid flow rate increases from 0.003L/Min to 0.011L/Min, the SMD decreases sharply. Then it increases obviously when the flow rate goes to 0.018L/Min. With the flow rate increasing, the SMD fluctuates and shows no dramatic changes.

It seems that flow rate increase has some impacts on atomizing effect, but not a wide range. In the actual working conditions, the flow rate should stay above a certain degree, otherwise the nozzle will not be in good function (Liu, 1998). In fact, each nozzle has a unique optimum working flow rate range. Liquid flow rate should be controlled within this range when the nozzle is working.

NUMERICAL SIMULATION

Mathematical Model

1. Particle Force Balance

In this article, we predict the trajectory of a discrete phase particle (or droplet or bubble) by

integrating the force balance on the particle, which is written in a Lagrangian reference frame. This force balance equates the particle inertia with the forces acting on the particle, and can be written (for the direction in Cartesian coordinates) as

$$\frac{du_p}{dt} = F_D(u - u_p) + \frac{g_x(\rho_P - \rho)}{\rho_P} + F_x \quad (3)$$

where F_x is an additional acceleration (force/unit particle mass) term, $F_D(u\text{-}u_P)$ is the drag force per unit particle mass and

$$F_D = \frac{18\mu}{\rho_P d_P^2}\frac{C_D \,\mathrm{Re}}{24} \quad (4)$$

Here, u is the fluid phase velocity, u, p is the particle velocity, μ is the molecular viscosity of the fluid, ρ is the fluid density, ρ, p is the density of the particle, and d, p is the particle diameter. Re is the relative Reynolds number, which is defined as

$$\mathrm{Re} \equiv \frac{\rho d_P \left|u_P - u\right|}{\mu} \quad (5)$$

2. The Discrete Random Walk (DRW) Model

In the DRW model, or "eddy lifetime" model, the interaction of a particle with a succession of discrete stylized fluid phase turbulent eddies is simulated. Each eddy is characterized by

·a Gaussian distributed random velocity fluctuation, u', v', and w'

·a time scale, τ_e

The values of u', v', and w' that prevail during the lifetime of the turbulent eddy are sampled by assuming that they obey a Gaussian probability distribution, so that

$$u' = \xi\sqrt{\overline{u'^2}} \quad (6)$$

where ξ is a normally distributed random number, and the remainder of the right-hand side is the local RMS value of the velocity fluctuations. Since the kinetic energy of turbulence is known at each point in the flow, these values of the RMS fluctuating components can be defined (assuming isotropy) as

$$\sqrt{\overline{u'^2}} = \sqrt{\overline{v'^2}} = \sqrt{\overline{w'^2}} = \sqrt{2k/3} \quad (7)$$

The characteristic lifetime of the eddy is defined either as a constant:

$$\tau_e = 2T_L$$

The particle eddy crossing time is defined as

$$t_{cross} = -\tau \ln\left[1 - \left(\frac{L_E}{\tau\left|u - u_P\right|}\right)\right] \quad (8)$$

Where τ is the particle relaxation time, L_E is the eddy length scale, and $\left|u - u_P\right|$ is the magnitude of the relative velocity.

The particle is assumed to interact with the fluid phase eddy over the smaller of the eddy lifetime and the eddy crossing time. When this time is reached, a new value of the instantaneous velocity is obtained by applying a new value of ξ.

3. Taylor Analogy Breakup (TAB) Model

The TAB model is a classic method for calculating droplet breakup, which is applicable to many engineering sprays.

The equation governing a damped, forced oscillator is

$$F - kx - d\frac{dx}{dt} = m\frac{d^2x}{dt^2} \quad (9)$$

where x is the displacement of the droplet equator from its spherical (undisturbed) position. The coefficients of this equation are taken from Taylor's analogy:

$$\frac{F}{m} = C_F\frac{\rho_g u^2}{\rho_l y} \quad (10)$$

$$\frac{k}{m} = C_k\frac{\sigma}{\rho_l y^3} \quad (11)$$

$$\frac{d}{m} = C_d\frac{\mu_l}{\rho_l y^2} \quad (12)$$

where ρ_l and ρ, g are the discrete phase and continuous phase densities, u is the relative velocity of the droplet, d is the undisturbed droplet diameter, σ is the droplet surface tension, and μ_l is the droplet viscosity.

$$x > C_b r \quad (13)$$

Where C_b is a constant equal to 0.5, if breakup is assumed to occur when the distortion is equal to half the droplet radius, i.e., oscillations at the north and south pole with this amplitude will meet at the droplet center. This implicitly assumes that the droplet is undergoing only one (fundamental) oscillation mode. Equation (9) is nondimensionalized by setting $y = x/(C_b r)$ and substituting the relationships in Equation (10) – Equation (11):

$$\frac{d^2y}{dt^2} = \frac{C_F}{C_b}\frac{\rho_g u^2}{\rho_l r^2} - \frac{C_k\sigma}{\rho_l y^3}y - \frac{C_d u_1}{\rho_l y^2}\frac{dy}{dt} \quad (14)$$

where breakup now occurs for y>1. For under-damped droplets, the equation governing y can easily be determined from Equation (14) if the relative velocity is assumed to be constant:

$$y(t) = We_c + e^{-(t/t_d)}[(y_0 - We_c)\cos(\omega t) + \frac{1}{\omega}(\frac{dy_0}{dt} + \frac{y_0 - We_c}{t_d})\sin(\omega t)] \quad (15)$$

Where,

$$We = \frac{\rho_g u^2 r}{\sigma} \quad (16)$$

$$We_c = \frac{C_F}{C_k C_b}We \quad (17)$$

$$y_0 = y(0) \quad (18)$$

$$\frac{dy_0}{dt} = \frac{dy}{dt}(0) \tag{19}$$

$$\frac{1}{t_d} = \frac{C_d}{2}\frac{\mu_1}{\rho_1 y^2} \tag{20}$$

In Equation (15), u is the relative velocity between the droplet and the gas phase, and *We* is the droplet Weber number, a dimensionless parameter defined as the ratio of aerodynamic forces to surface tension forces. The droplet oscillation frequency is represented by ω.

Geometry Model Design and Mesh Generate

Geometry model of the spray chamber is shown in Figure 6 and Figure 7. Its structure consists of a spray chamber, an inlet section and a stable segment. Fundamental purpose of the design is to mix the air and atomized particles as fully as possible to make sure the atomized particles distributed as evenly as possible in the stable segment. Size of the spray chamber is 1400mm×1400mm×2400mm, the radius of the inlet section is 400mm. Cross-section of the stable segment is a round face with 200mm radius and length of the stable segment is 2400mm. In this paper, unstructured grid is used to discrete computational domain, the grid number is 1.8 million, as in Figure 8.

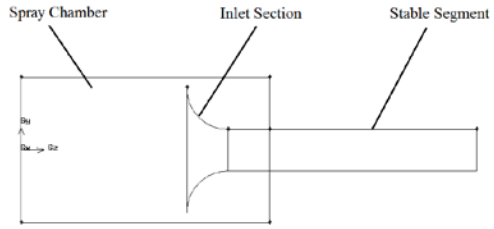

Fig. 6. Side view of the spray chamber geometry

Nozzle arrangement schemes:

To find out impact of number and arrangement of the nozzles on particle distribution uniformity in atomized field, four different layout schemes have been designed (An, 2003). Fig. 7 shows names of different faces.

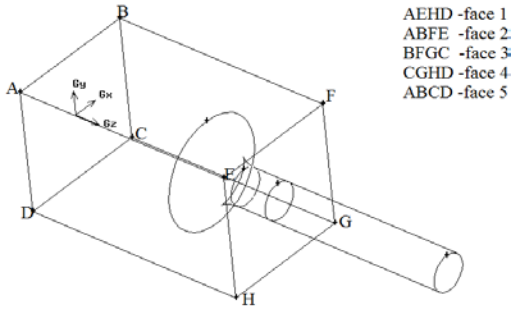

Fig. 7. A perspective view of the spray chamber geometry

Scheme 1:

Four nozzles are all set in face 5;

Scheme 2:

Eight nozzles, four in face 5, one in face 1, face 2, face 3 and face 4 each.

Scheme 3:

Twelve nozzles, four in face 5, four in face 1 and face 3 each.

Scheme 4:

Twelve nozzles, four in face 5, two in face 1, face 2, face 3 and face 4 each.

Mesh generation:

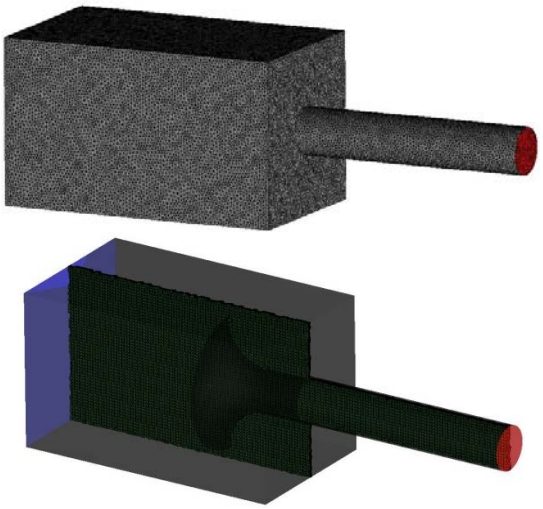

Fig. 8. Mesh of the flow field

Calculation Configuration:

In the calculation, continuous flow field is calculated first. Then the Discrete Phase Model is used for coupling calculation. Outlet pressure is set as -120Pa, time step size is 0.001s, and the maximum number of iterations steps is 20. The k-ε model is used in steady flow field calculating. Experimental data of particle size distribution is set as part of boundary conditions and calculated in the simulation process.

Results and Analysis

Velocity field flow chart of a typical cross section in spray chamber is shown in Figure 9. The flow characteristics are shown clearly.

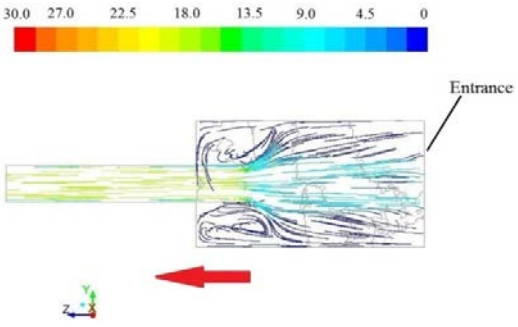

Fig. 9. Velocity flow chart of the middle section

From the figure, the whole flow field can be divided into four parts approximately. In the area

near the entrance, the entire flow field is relatively uniform. The overall speed in this section is relatively low, velocity values are mostly below 10m/s. The second part is the area near the curved inlet section. Due to contraction of the inlet-section, part of the air flow changes its direction violently (Zhang, 2006). The third part is the area behind inlet section, vortex appears because of the clogging and irregular shape of the flow path. The fourth part is the area in the stable segment, as shown in the flow chart, the air flow is relatively stable, but with higher speed. Although the flow field is somehow disordered because of the inlet section, its curved design makes the subsequent flow field maintain in a relatively stable state (Cao, 2005). From the flow chart, apart from the area around the inlet section, the overall flow field is very stable which meets the practical requirements.

Figure 10 shows the particle trajectories of a typical nozzle layout scheme in the entire flow field.

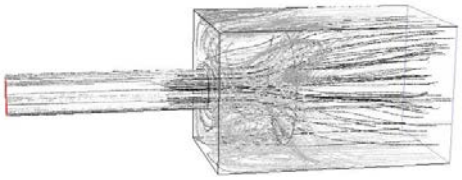

Fig. 10. Distribution of particle trajectories

In the study of spray field, the droplets produced in the spray are processed by the Discrete Phase Model (DPM) (Wang, 2004). By using the Discrete Phase Model that CFD software provides, Lagrange equations can be used to calculate the discrete phase trajectory (Cui, 2006). Turbulent eddies effects on the droplet particles can be predicted. In addition, droplet evaporation process, boiling process, heating process, burst process, merging process and other types of discrete phase, like cooling process, continuous phase and discrete phase coupling process, can all be reflected in the calculation (Rao et al., 1976). During the coupling calculating of the discrete phase and the continuous phase (Liu et al., 2005), the movement of continuous phase will impact discrete phase, and vice versa (Hou, 2005). From Fig. 10, droplets move in vortex together with the air.

Based on the calculation results, the Maximum concentration, Average concentrations in different sections are obtained. In this paper, the concentration non-uniformity is defined as follow,

$$\delta = \frac{C_{\max}}{C_a}$$

δ represents concentration non-uniformity, $C_{\max}$ represents the maximum concentration in the section, C_a represents the average concentrations.

Figure 11 shows the particle non-uniformity results of the four diffident schemes. The horizontal axis represents dimensionless position.

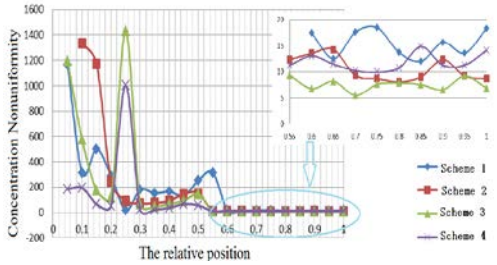

Fig. 11. Non-uniformity of the concentration in four different schemes

In these four schemes but the first one, the non-uniformity along varies violently in different positions. This is mainly because of arrangement forms of the nozzles (Hou, 2012).

In scheme 1, the nozzles are all placed on the entrance wall. Therefore, particle distribution can remain relatively stable in most of the area. In scheme 2, on the contrast, there is only one nozzle on each circumferential wall. That is why there is a crest in the graph (Gan, 1990). Other schemes show the same pattern. After the fluctuation, an arch occurs in all four curves. These regions in the curves correspond to the trumpet-shaped inlet section, in which scheme 1 has the highest non-uniformity and scheme 4 has the lowest one (Shen, 2000). When the air flow into the stable segment, the distribution of concentration becomes uniform and the four curves have leveled off.

By contrast Scheme 1 (4 nozzles), Scheme 2 (8 nozzles) and Scheme 4 (12 nozzles), increasing nozzle number can help to keep the concentration non-uniformity of droplets of the spray chamber in a reasonable range (Han, 2010).

Although the nozzles in Scheme 4 are arranged more dispersed (Wang, 2008), the concentration non-uniformity in the stable segment is still higher than that in Scheme 3. This is because the turbulence flow around the inlet section has helped the droplets to disperse and improve uniformity (Li, 2007).

CONCLUSIONS

In this paper, experiment study and numerical simulation are used to test function of the air atomizing nozzle and analyze performance of the artificial seawater spray chamber. Main purpose of the test is to obtain performance data of the nozzle which will be used in the calculation of the spray chamber. By analyzing the results of these studies, nozzles performance in variable conditions and flow field in the spray chamber are obtained.

(1). Experimental results show that, spray angle does not change apparently with variation of pressure. Therefore, main factors which affect nozzle spray angle are not its operating parameters, but its structural parameters.

(2). Results show that pressure is one main factor that affect the atomizing effect. Increasing the pressure in a reasonable range can improve atomization performance. Though increasing fluid flow rate will affect the atomization effect, atomizing nozzle performance does not change apparently with the increase of the fluid flow rate.

(3). Comparing different schemes, effects of the nozzle numbers and nozzle arrangement method on the spray field uniformity have been obtained. higher nozzle number can make the concentration distribution in the spray chamber more uniform.

ACKNOWLEDGMENT

This work is funded by the Fundamental Research Funds for Central Universities, No. HEUCF150305, also supported by the National Natural Science Foundation of China (NSFC) [No. 51509052]. It is also financially supported by the Institute of Purification and Separation Technology, Harbin Engineering University, Heilongjiang, China.

REFERENCES

An Hui, "Experimental Study on inner recirculation two-fluid residue atomizing nozzle," *Dalian University of Technology*, Dalian (2003).

Bulzan D L, "Velocity and drop size measurements in a confined, swirler-stabilzed, combusting spray," AIAA, 96-3164, (1996).

Cai J and Jeng S M, "The Structure of a Swirl-stabilized Reacting Spray Issued from An Axial Swirler," AIAA, 2005-1424, (2005).

Cao Mingjie, "Spray study" Machinery Industry Press, Beijing, (2005).

Cui Yandong, "Study on mechanism of pneumatic atomizing nozzle and development of coal-water slurry gasification nozzle," Zhejiang university, Zhejiang (2006).

Fu Y Cai J Jeng S-M and Mongia H C, "Fuel and Equivalence Ratio Effects on Spray Combustion of a Counter-Rotating Swirler," AIAA, 2005-0354, (2005).

Fuster, Daniel, et al. "simulation of primary atomization with an octree adaptive mesh fefinement and VOF method," *International Journal of Multiphase Flow.*, p35, (2009).

Gan Xiaohua, "Model and calculation of air atomizing nozzle," *Aerospace Power*., (1990).

Gan Xiaohua, "Aviation turbine fuel nozzle technology," Defense Industry Press, Beijing, (2006).

Han Zhanzhong, "FLUENT fluid engineering simulation and application examples (2nd Edition)" Beijing Institute of Technology Press, Beijing, (2010).

Hou Linyun, "Nozzle Technical Manual" China Petrochemical Press, Beijing (2002).

Hou Yan, "Numerical simulation of multi-nozzle spray field," *Chinese Journal of Engineering Thermophysics*., (2012).

Jeng S M Flohre N M and Mongia H C, "Swirl Cup Modeling Atomization," AIAA 2004-137(2004).

Li Hongjun, "The study of Gas-particle two-phase flow field characteristics in Artificial seawater spray chamber," Harbin Engineering University, Harbin, (2006).

Li Ping, "CFD simulation of two-phase flow field in mixed air atomization of diesel nozzle," Nanjing University, Nanjing (2007).

Liao, Y., Jeng, S. M., Jog, M. A., & Benjamin, M. A, "An Advanced Sub-model for Air-blast Atomizer," AlAA,99, (2007).

Liu Yingzheng, "Phase doppler particle technology issues in measurement applications," *Ship Engineering*., (1998).

Liu Liansheng, Hua Yang, Jinxiang Wu, "Breakup process and spray characteristics of effervescent atomization with the annular outlet," *Combustion Science and Technology*., 11(2):121-125, (2005).

Ma Shuzhe, Shuping Tu, Shouguang Yao, "Numerical simulation of gas-liquid two-phase flow and combustion in Venturi-type oil burner outlet," *East China Shipbuilding Institute Journal.*, 2001-15(1):77-81, (2001).

Rao, K. V. L., & Lefebvre, A. H. "Evaporation characteristics of kerosene sprays injected into a flowing air stream," *Combustion and Flame*., 26:303-309, (1976).

Shen Xiong, "Atomized droplets and flow characteristics measuring by using phase doppler laser system," *Hydrodynamic experiments and testing*., (2000).

Soltani, M. R., Ghorbanian, K., Ashjaee, M., & Morad, M. R. "Spray characteristics of a liquid-liquid coaxial swirl atomizer at different mass flow rates," *Aerospace Science and Technology*,592-644, (2005).

Sun Haiou, "The impact of spray on gas-particle two-phase flow field in the artificial seawater spray chamber," *Applied Science and Technology*, (2006).

Tambe S B and Jeng S M, "Liquid Jets in Subsonic Crossflow," AIAA,2005-731, (2005).

Wang Fujun, "Computational fluid dynamics analysis-CFD Software Principles and Applications," Tsinghua University Press, Beijing, (2004).

Wang Li, “Experimental study on atomization quality of aviation engine fuel nozzles and simulation flame tube,” *Shenyang Institute of Aeronautical Journal*, Shenyang, (2008).

Zhang Shurong, “Characteristics of air-atomizing nozzle,” Dalian University of Technology, Dalian, (2006).

Zhang Shurong, “The study on characteristics of air-atomizing nozzle,” Dalian University of Technology, Dalian, (2006).

Zheng Wenjie, “Modeling and simulation study on low pressure atomizing nozzle with low viscosity and small flow of fluid,” Shanghai Jiaotong University, Shanghai, (2010).

Zhang Zheng, “The study of fuel atomization field characteristics in the combustion chamber,” Nanjing University of Aeronautics and Astronautics, Nanjing, (2009).

人工海水霧化室流場特性研究

李良才 殷越 萬博 欒一剛
哈爾濱工程大學動力與能源工程學院

摘 要

進氣濾清器在燃氣輪機中有著極其重要的位置，而噴霧條件又影響著其設計可靠性。因此，為了更好的對燃氣輪機進氣濾清器進行研究和設計，需要按照實際需求為其設計某種形式的人工海水霧化室，以便模擬海洋大氣環境。在人工海水霧化室中，噴嘴為後續霧化提供了必要初始條件，霧化場的均勻性與噴嘴類型、數量、佈置位置等參數密切相關。霧化室的設計通常是基於實心圓錐噴嘴技術。通過一定的方式及規律佈置噴嘴，並結合與之相配的霧化室機構就可以設計出滿足一定需要的霧化室。人工海水霧化室一般需要滿足液滴霧化後霧滴均勻性的要求。在計算流體力學技術迅速發展的今天，通過通用的 CFD 軟體，結合一定的試驗資料，對霧化立場進行整體模擬計算，可以為整個霧化室的設計提供較為可靠的依據。本文將先利用 PDA 技術，對噴嘴性能進行試驗研究，得到相關的實驗資料。然後建立霧化室幾何模型，並將得到的噴嘴資料帶入邊界條件進行計算，對設計的霧化室進行研究並優化。